1-1-2020

# Development Of A Liposomal Formulation For Brain Targeting

Ziru Zhang

# DEVELOPMENT OF A LIPOSOMAL FORMULATION FOR BRAIN TARGETING

A Thesis

Presented for the

Master of Science Degree

The

Department of Pharmaceutics and Drug Delivery

The University of Mississippi

by

ZIRU ZHANG

May 2020

## ABSTRACT

The blood-brain barrier (BBB), formed by the endothelial cells of the brain capillaries, inhibits the penetration of many therapeutic compounds into the brain. Liposomes, which have unique physicochemical characteristics, have been widely investigated for the drug delivery system across BBB. In the current study, FITC-dextran was used as a model drug that encapsulated in a liposomal formulation to investigated its ability to overcome the blood-brain barrier for targeted brain delivery of therapeutic agents.

Here, non-targeted liposome (NT LPs) and RVG-modified liposome (RVG LPs) were prepared. The NT LPs and RVG LPs were about 97 and 101 nm in diameter with the zeta potential of -27.0 mV and -21.2 mV, respectively. *In vitro* study in mouse SH-SY5Y neuroblastoma cells and mixed glial cells demonstrated that the RVG LPs were taken up with enhanced efficiency comparing to the NT LPs. *In vitro* release study results indicated the sustained release of FITC-dextran from NT LPs. A preliminary pharmacokinetic study showed prolonged circulation time of FITC-dextran encapsulated in NT LPs compared to the free form. As expected, free FITC-dextran manifested no brain distribution. Further studies on the pharmacokinetics of RVG LPs are warranted, to establish the proof of concept for its application in brain-targeted drug delivery.

## ACKNOWLEDGMENTS

I would like to thank my advisor, Dr. Chalet Tan, for supporting my projects. When I first came to this lab, I was totally a “newbie” in research and lacking experience. She always patiently encouraged me and guided me when I lost. She made herself an example to let me know what is the real research, as well as being critical and accurate all the time. And thank Dr. Jason Paris and Ms. Fakhri Mahdi for their support in my study. They always give me some advice which is so valuable to help me think differently. Also, thanks to Dr. Walter G. Chambliss, for being part of my committee members, his formulation course was the first step for my master study and gave me a lot of guidance on my project.

I also would like to thank my seniors and colleagues, Sheng Feng, Nan Ji, Minjia Wang, Yusheng Li, Pranav Ponkshe and Nidhi Dineshkumar Patel for helping me with my experiments.

Finally, I thank my family for supporting and encouraging me through my study.

## TABLE OF CONTENTS

## LIST OF FIGURES

## LIST OF TABLES

# I. INTRODUCTION

Brain diseases have a huge impact on the safety and quality of human life because of its high morbidity and mortality[1]. According to statistics, the USA and Europe spent about 800 billion dollars on brain diseases in the past ten years[2]. However, the development of the therapeutics for brain diseases is slow and immature compared to other therapeutic areas. A crucial challenge of the treatment for brain diseases is the complex microvasculature. The blood-brain barrier (BBB) is located between a blood vessel wall. It is a semi-permeable membrane in the central nervous system (CNS) and it is mainly comprised of tightly sealed brain capillary endothelial cells that are surrounded by astrocytic perivascular end-feet and pericytes through the basal lamina (Figure.1A). Pericytes which are covering 20% of the outer surface of endothelial cells can control the blood flow in the brain capillary by contraction and relaxation. Astrocytes are glial cells connect the brain capillary and neurons. The previous studies showed that astrocytes played an important role in BBB's barrier integrity. Both pericytes and astrocytes can provide neurons with nutrition to maintain BBB's function, therefore, avoiding oxidative stress and metal toxicity. The endothelial cells limit the diffusion of molecules and proteins because they do not have fenestrations. There is a high electrical

resistance (1500–2000 Ω $cm^2$) within the endothelial cells caused by the encapsulation of capillaries by the pericytes and astrocytes that only allow the small molecules to penetrate through passive diffusion. The tight junction is the main component with high trans-endothelial resistance in the BBB. They severely restrict paracellular diffusion of the water-soluble agents[3,4]. As the results of these barriers, only small (molecular weight < 400 Da), lipid-soluble molecules can cross the BBB by passive diffusion, however, most molecules with characteristics such as high molecular weight, high electric charge or hydrophilicity cannot pass through BBB. This structure of BBB protects it from harmful foreign substances; however, it blocks 95% of potential drugs from entering brain[5,6].

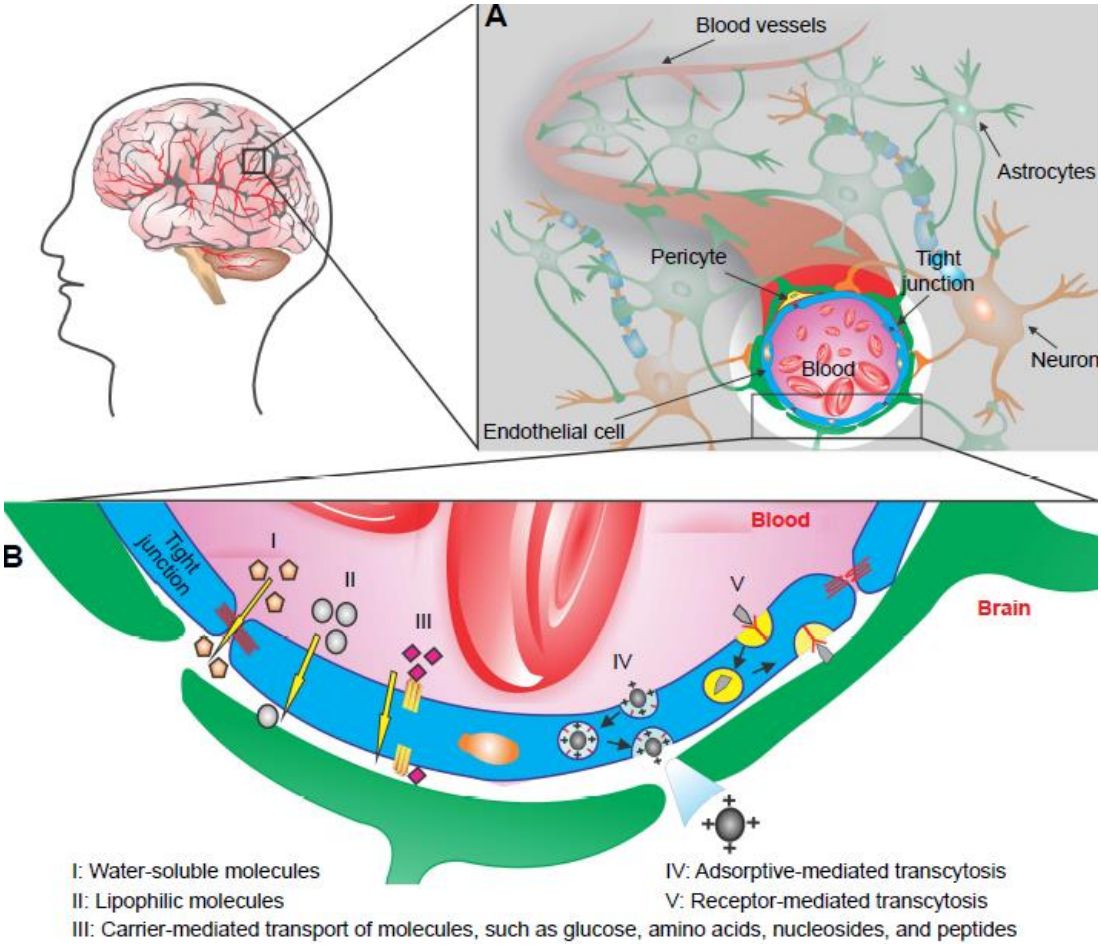


**Figure 1.** Anatomy and pathways for crossing the Blood-Brain Barrier (BBB).
The BBB is located at the walls of the blood vessels that supply the central nervous system, including the brain. (A) Cross-section of a cerebral capillary. (B) Different mechanisms for

drug delivery across the BBB.

In general, the mechanism of the solute transcellular pathway through the BBB are divided into three groups: passive diffusion, carrier-mediate transport, and endocytosis (Figure.1B). Passive diffusion is driven by the concentration gradient between both sides of the membrane without the consumption of ATP, this makes some water-soluble molecules and small lipophilic molecules able to pass through BBB. The size, polarity, and lipophilicity of a substance are the factors which can influence the rate of passive diffusion[7]. However, passive diffusion is rare in the process of substance transport across BBB. In most cases, the peptides and small molecules pass through the specific carrier-mediated transport. Some ions, glucose, nucleotides, etc. are diffused into the membrane with the help of transport proteins on the endothelial cells[6]. This kind of transportation has three characteristics: 1. Substances can be transferred against the concentration gradient. 2. The specific receptor is needed. 3. ATP is needed through the whole procedure[8].

Transcytosis of macromolecules across BBB provides the main route by which large molecular weight solutes enter the CNS intact[8]. Initially, the endocytosis mechanism is an invagination of the plasma membrane that leads to the production of endocytic vesicles which facilitated the incorporation of extracellular macromolecules into the cells[9]. Receptor-mediated transcytosis can provide a specific uptake of the extracellular macromolecules which has been well studied for brain targeting. Endothelial cells have different receptors for various types of ligands' uptake. Macromolecules first bind to receptors known as coated pitsthat which collected in specific areas of the plasma membrane. These pits invaginate into the cytoplasm and then pinch free of the plasma membrane to form

coated vesicles after bound to the ligand. After acidification of the endosome, the ligand will dissociate from the receptor and cross the other side of membrane[10,11].

Liposomes are sealed vesicles with a bilayer structure. The bilayer composes of amphiphilic molecules such as phospholipids. Therefore, liposomes can encapsulate both water-soluble and lipid-soluble substances[6]. Considering that conventional liposomes are mainly constituted of lipids and amphiphilic phospholipids, liposome's lipophilic layers facilitate the drug passing across the membrane of brain endothelial cells liposomal formulations can which endow excellent features for transporting drugs to the BBB and release their content following endocytosis to permit encapsulated drugs to gain access to the brain. Due to it have so many advantages, its' good biocompatibility and biodegradability, high delivery efficiency and flexible modification strategies, liposomes were expected to be ideal carrier for brain drug delivery. for brain uptake[12]. The conventional liposomes can carry a drug cargo into the brain by the mechanism of endocytosis.

However, there are still some issues that hinder the brain targeting and tissue distribution. The fast clearance of the liposomes leads to a restricted circulation time and a reduced BBB crossing ability[13].

The stealth technology of liposomes is to functionalize a liposome's surface with polyethylene glycol (PEG) or polysaccharides. In this way, stealth liposomes protects the active moiety from the recipient's immune system, which results in reduced immunogenicity and antigenicity.[14] Longer circulation time-period and more tissue distribution can be realized thereby increasing the liposome's targeting efficiency[12,14,15].

Doxil® is a liposome which was first approved by FDA as a nano drug delivery system

based on PEGylated liposome technology through intravenous injection. Doxil® liposomes are composed of HSPC, cholesterol, and DSPE-PEG. More drug retention was obtained because of the optimum proportion of cholesterol and HSPC, which forms a non-flexible bilayer at 37℃ and below 37 ℃, this loading technology allows higher retention with less drug efflux in circulation, while providing acceptable rates of drug distribution in tissues [14].

So, in this study, HSPC, cholesterol, DSPE-$PEG_{2000}$ was used as the composition of NT LPs' lipid. For RVG LPs, DSPE-PEG-RVG was synthesized by coupling RVG-peptide to DSPE-$PEG_{2000}$ instead of DSPE-$PEG_{2000}$.

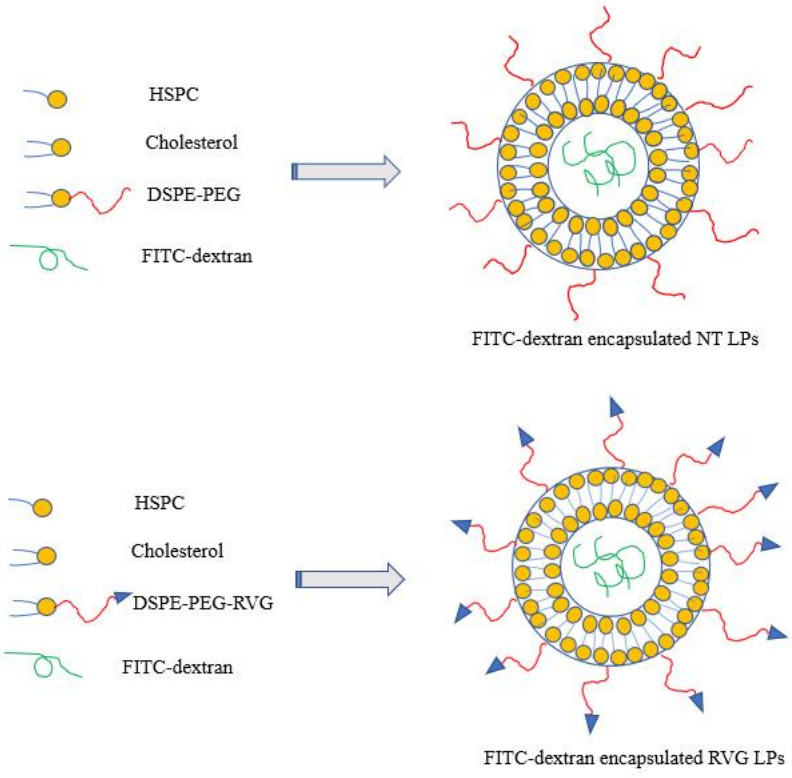


**Figure 2.**. Structure of FITC-dextran encapsulated NT LPs and RVG LPs.

Surface-functionalized liposomes with a wide variety of targeting agents can achieve effective delivery across the BBB and can be designed to interact with specific therapeutical

targets and finally arrive at the targeted site in brain[1,16]. RVG is a 29-amino acid peptide derived from rabies virus glycoprotein[17]. It can bind with the α7 subunit of nicotinic acetylcholine receptor (nAchR)[18]. Since microglial cells of BBB express nAchR widely, RVG can interact with microglial specifically, thereby entry into BBB[19]. The ability of RVG to enter the brain through the BBB via intravenous injection has been demonstrated by previous experiments. Moreover, RVG promotes retro-axonal and the spread of trans-synaptic thereby enhances the transduction of neighboring neuronal cells[20]. Compared with the large molecule protein ligands or antibodies, peptide ligands such as RVG have several advantages: (1). Easy synthesis and isolation (2). Low immunogenicity and (3). Stable during the process of coupling to the nanoparticles[21]. In this way, due to the ability demonstrated by RVG-conjugated nanoparticles to overcome the BBB through nAchR-mediated endocytosis and promote the preferential accumulation of loaded nucleic acid in neuronal cells, RVG ligand was chosen to functionalized the liposome's surface for enhanced BBB penetration and brain targeting[19]. So, in this study, simple "none-targeted" liposomes and RVG modified liposomes were prepared, and different characteristics of the liposomal formulation were studied (Figure 2).

Liposomes' ability of drug-carrying and transport capabilities can be investigated by *in vivo* imaging markers, such as fluorescent dyes for optical imaging[7]. The selected fluorescent dyes when assessing BBB permeability requires: (1). The fluorescent dye cannot penetrate

the BBB naturally, (2). It should be quantifiable in low concentrations[22], and (3). It should not affect the physiology and function of the animals. Also, since the process of the fluorescent dye going into the liposomes is not an “all-or-nothing” phenomenon, the molecular size of the tracers needs to be taken into consideration. Typically, if higher molecular weight tracers with the complex chemical structure are encapsulated in liposomes, the liposome is considered to have better loading efficiency than that only the low molecular weight tracers can be encapsulated[23]. Fluorescein isothiocyanate dextran (FITC-dextran) is a large water-soluble molecule that is widely employed to assess BBB permeability in this century[24]. The solubility of FITC-dextran in water at concentrations at or above 25 mg/ml. Considering all of the necessary conditions for *in vivo* image markers mentioned above, in this study, the FITC-dextran was utilized as a model drug to investigate the delivery effect of the liposomal formulations.

In this work, FITC-dextran encapsulated NT LPs and RVG LPs were prepared. Particle size, zeta-potential and stability of the liposomal formulations were studied. *In vitro* uptake of each liposome formulation was evaluated in SH-SY5Y neuroblastoma cells and primary brain mixed glial cells. Then, *in vitro* release study demonstrated an extended release of FITC-dextran encapsulated liposome. Lastly, the pharmacokinetics of FITC-dextran-loaded NT LPs was studied in mice following IV injection and the brain distribution was evaluated.

## II. MATERIALS AND METHODS

### Chemicals and instrumentation

Hydrogenated soybean phospholipids (HSPC, MW: 783.774), 1,2-distearoyl-sn-glycero-3 phosphoethanolamine-N- [methoxy (polyethylene glycol)-2000] (DSPE-$PEG_{2000}$, MW: 3400) were purchased from Avanti Polar Lipids, INC. (AL, USA). Cholesterol (MW: 386.654) was purchased from MP Biomedicals, LLC. (OH, USA). Fluorescein isothiocyanate (FITC)-dextran (100 kDa) was bought from Sigma–Aldrich (MO, USA). Trichloroacetic Acid was purchased from VWR International LLC. (PA, USA). Sodium Hydroxide was purchased from Fisher Scientific (NJ, USA). Tris was bought from MARESCO Inc. (OH, USA). Triton® X-100 was bought from Sigma–Aldrich (MO, USA). DSPE-PEG-RVG (MW: 7092.5) was synthesized by coupling RVG-peptide to DSPE-PEG2000. ICR (CD-1) mouse was purchased from ENVIGO.

Treated cells were imaged by a fluorescence microscope (Nikon Instruments Inc., Melville, NY). Fluorescent detection was performed on CLARIOstar® Plus microplate reader (BMG LABTECH, Germany). The average size, polydispersity index (PDI) and zeta potential were determined using Nano ZS zeta sizer (Malvin, UK).

**Preparation of the NT LPs and RVG LPs**

The liposomes were prepared by a thin-film method[25]. NT LPs with the composition of HSPC, cholesterol, and DSPE–$PEG_{2000}$ at 67.5: 30: 2.5 (mol) ratios were prepared[26]. Briefly, 0.5mg of lipids were mixed and dissolved in 300 µl chloroform in a round-bottom flask, which was removed under vacuum at room temperature to form a homogenous thin lipid film. The lipid film was hydrated at 60 ℃ with 5mM FITC-dextran solution, then sonicated for 2 h under 60 ℃ water bath.

The NT LPs encapsulated with FITC-dextran were separated from non-encapsulated FITC-dextran by passing the liposomal solution through an ultrafiltration filter (Amicon® Ultra Centrifugal Filters, 100K MWCO). The resultant liposome solution was stored at 4 ℃. In addition, RVG LPs were prepared using the same method described above, except that 0.6 mg of lipids were mixed and dissolved in 200 µl of chloroform and 100 µl of acetonitrile-methanol (1:1, v/v).

**Characteristics of the liposomes**

NT LPs and RVG LPs' properties, particle size, PDI and zeta potential were measured by a Dynamic Light Scattering (DLS) analyzer (Nano-ZS; Malvern, UK).

The concentration of encapsulated FITC-dextran in the liposomes was determined by fluorescent detection conducted on CLARIOstar® Plus microplate reader (BMG Labtech INC, USA). The excitation and emission wavelengths were 493 nm and 520 nm, respectively. Before the fluorescent detection, the liposomal formulation was lysed by adding 1% Triton® X-100 solution to each sample followed by 15 minutes of a continuous vertexing to eliminate

the interference of lipid and quantify the total amount of encapsulated drug[27]. The drug encapsulation rate percentage (ER%) of liposomes and drug loading percentage (DL%) of liposomes (LPs) was calculated by the equations below:

$$(ER\%) = \left(\frac{Drug\ in\ the\ LPs}{Total\ drug}\right) * 100\%$$

$$(DL\%) = \left(\frac{Weight\ of\ drug\ in\ LPs}{Total\ weight\ of\ LPs}\right) * 100\%$$

**Stability study**

The freshly prepared liposomes were stored at 4 °C. Size and drug leakage of the liposomal formulation were monitored for up to two weeks upon storage in DI water at 4 °C. The released FITC-dextran was removed by passing the liposomal solutions through the Amicon® Ultra spin filters (100K MWCO) by centrifuging at 2000 x g at 4 °C for 15 min.

**Cell uptake study**

The SH-SY5Y neuroblastoma cells were purchased from ATCC and were used only up to passage number 20. Primary mixed glial cells were prepared from the pups (0-1 day) of ICR (CD-1) mouse and seeded at 220,000 cells per well of poly-L-lysine treated 24 well plates. The cells were grown for 8 days followed by treatment with liposomes (NT, RVG LPs, and free FITC dextran)

On the day of the assessment, the media was removed and the cells were washed with HBSS once. A working solution of propidium iodide (ex/em: 536/617 nm) and Hoescht 33342

(ex/em: 350/461 nm) was prepared by diluting stocks in Hank's Balanced Salt Solution (HBSS; 1:50 dilution for propidium iodide and 1/10000 for Hoescht). Fluorophores-containing HBSS (300 µl) was added to each well. The cells were incubated for 15 min at 37 ℃ humidified incubators with 5% $CO_2$ and followed by reading on a CLARIOstar® plate reader (BMG Labtech, NC). After reading the cells in the plate reader, the cells were imaged using a Ti2-E motorized, mounted with 40,6-diamidino-2-phenylindole (DAPI) and observed with a microscope (Nikon Instruments Inc. NY) to check the uptake of each type of liposomes.

**Quantification of FITC-dextran**

The calibration curves for FITC-dextran in DI water, plasma, and brain homogenate were established by spiking the FITC-dextran stocks (1 mM) with a range of 0.005-5 µM, 0.01-0.1µM, and 0.03-0.5µM, respectively.

The plasma and tissue homogenate samples were analyzed by protein precipitation method using trichloroacetic acid[28]. The mice's brain tissue was dissolved in PBS buffer (1:1, v/v) and homogenized by probe sonication. Briefly, 100 µL trichloroacetic acid (50%, w/v) were dropwise added to plasma and tissue homogenate samples, and the suspended solution was centrifuged at 4000×g at 4 ℃ for 5 min. The supernatant was collected and neutralized with 10M NaOH and Tris-based buffer (pH=8) for fluorescent analysis. All the samples were detected via spectrophotometry (fluorescein-dextran: 493/520 nm, ex/em).

***In vitro* release study**

The *in vitro* release kinetics of free FITC-dextran and NT LPs were studied in phosphate

saline buffer (PBS, 20 mM pH 7.4) and fetal bovine serum (FBS, Invitrogen, Carlsbad, CA) using a dialysis method[29]. The liposomes were prepared as described before and diluted 10 times with PBS or FBS. Free FITC-dextran and NT LPs were loaded into a 200 µl Micro Float-A-Lyzer (100K, Fisher Scientific, NJ). Each cassette was placed in 500 ml PBS to ensure the sink condition. The release medium was refreshed every 2 h. At each time point, samples were collected from the dialysis cassette. The concentration of each sample was determined by the CLARIOstar® plate reader (493/520 nm, ex/em).

**Pharmacokinetics of free FITC-dextran and NT LPs**

The mice were randomly divided into two groups (n=3) for the pharmacokinetic study of free FITC-dextran and NT LPs. The free FITC-dextran group and NT LPs group were administered via *i.v.* route at 2 mg/kg. Whole blood samples were collected via the retro-orbital bleeding at predetermined time points after administration. The plasma was obtained by centrifuging the blood sample at 4800×g for 5 min for further analysis. The plasma samples were analyzed using the protein precipitation method previously described.

**Brain distribution study**

To determine the biodistribution of free FITC-dextran, mice were randomly divided into 2 groups (n=3). Each group of mice was intravenously injected with PBS, free FITC-Dextran at a dosage of 8 mg/kg.

The brains were harvested at 80 minutes and were processed for the further analysis described above.

## III. RESULTS

### Characteristics of the liposomes

The size distribution of liposomes can influence the release, cell uptake, and biodistribution. The particle size and surface charge of liposomes are summarized in Table 1 and Figure 3. The NT LPs had a mean size between 97.3 ± 4.02 nm, and the RVG LPs had a mean size between 101.9 ± 2.38 nm. Both of them had a PDI below 0.2 which indicated a uniform spherical nanoscale liposome was formed as expected. Since the ability of liposomes to cross the BBB is at least partially dependent on their size, the achieved sizes smaller than 200 nm met the requirements for a potentially successful BBB targeting. Liposomes being too small (size < 50 nm) may escape out of peripheral capillaries, while liposomes being too large (size > 200nm) may not be able to pass cell membranes and may be removed faster by the reticuloendothelial system (RES). Particles below 200 nm rather avoid recognition by the RES and exhibit a prolonged half-life in the blood[30].

The zeta potential of NT LPs and RVG LPs were -27.0 mV and -21.2 mV, respectively, which showed both NT LPs and RVG LPs were negatively charged.

The drug encapsulation rates (ER%) of NT LPs and RVG LPs were 0.29 ± 0.01%, 0.15 ± 0.025%. The drug loadings (DL%) of NT LPs and RVG LPs were 6.11± 1.2% and 1.93 ± 0.9%,

respectively. Since the model drug, FITC-dextran, is a large hydrophilic molecule with a long chain chemical structure. The drug encapsulation rates and drug loading percentage was acceptable. Future formulation of the drug with lower molecular weight and simplified chemical structure was anticipated to have higher drug encapsulation rates and drug loading percentage.

**Table 1.** Particle size (nm) and surface charge of NT LPs and RVG LPs.

| | Particle size (nm) | PDI | Zeta potential (mV) |
|---|---|---|---|
| NT LPs | 97.3 ± 4.02 | 0.108 | -27.0 ± 5.91 |
| RVG LPs | 101.9 ± 2.38 | 0.071 | -21.2 ± 5.60 |

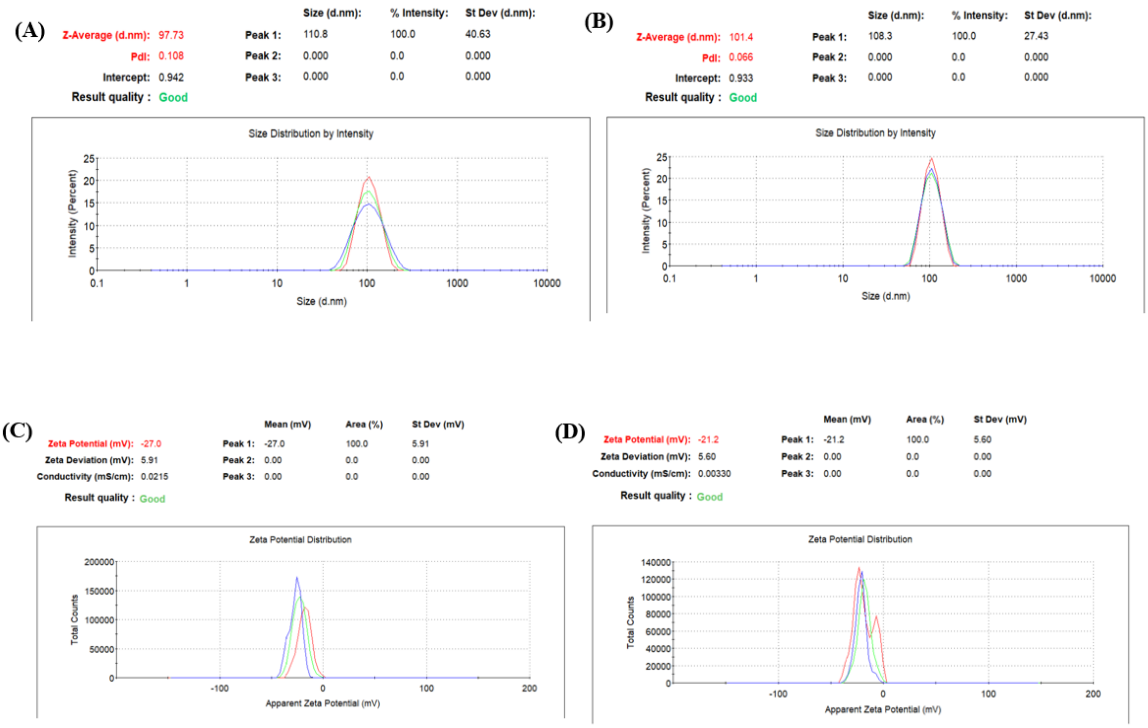


**Figure 3.** The particle size (nm) and zeta-potential of NT LPs and RVG LPs. (A) NT LPs' particle size. (B) RVG LPs' particle size. (C) NT LPs' zeta-potential. (D) RVG LPs' zeta-potential.

## Stability study

The stability of the NT and RVG LPs storage in DI water was tested by monitoring the particle size and the concentration of encapsulated FITC-dextran (Figure 4). The results showed that for both NT and RVG LPs' the drug concentration loss was less than 15%, and their size loss was less than 5%, which demonstrates both formulations were stable at 4 ℃ for 14 days.

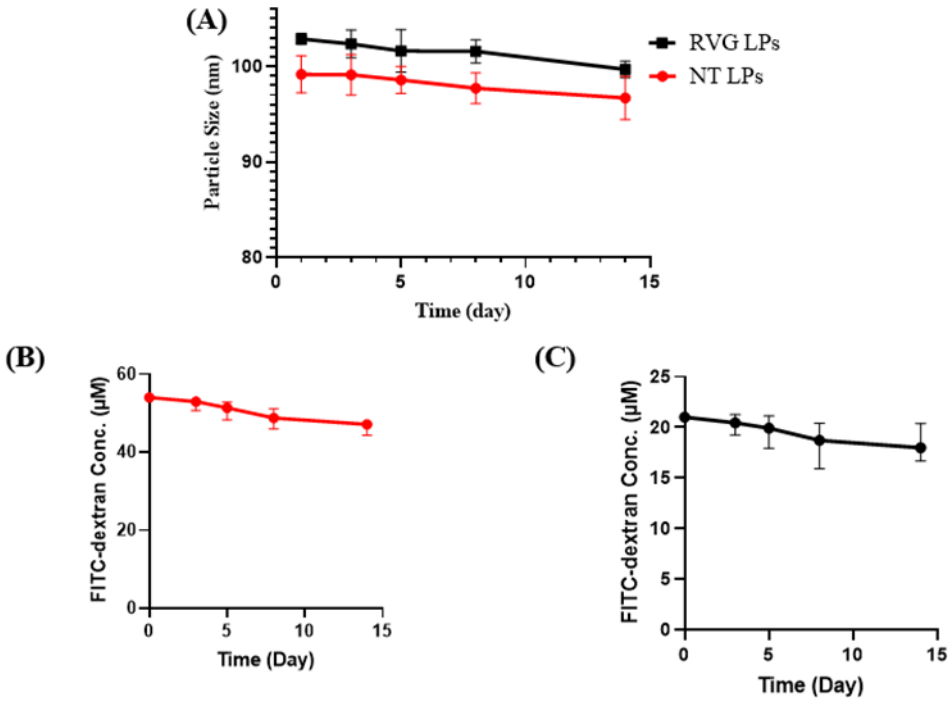


**Figure 4.** Stability study of NT LPs and RVG LPs for 14 days storage in DI water at 4 ℃. (A) The particle size of NT LPs and RVG LPs. (B) The concentration of encapsulated FITC-dextran in NT LPs. (C) The concentration of encapsulated FITC-dextran in RVG LPs.

## Cell uptake study

To investigate the internalization and intracellular behavior of FITC-dextran loaded liposomes, cellular uptake was examined after 48-hour treatment of free FITC-dextran, NT LPs, and RVG LPs using a fluorescence microscope. As shown in the microscope images (Figure 5), a similar intensity of DAPI staining in the wells of each cell type demonstrate the

uniform seeding of the primary culture. Low green fluorescence could be detected in NT LPs treated cells, by contrast, strong green fluorescence was observed in the cells treated with RVG LPs, demonstrated enhanced uptake of RVG LPs by the SH-SY5Y neuroblastoma cells and mixed glial cells.

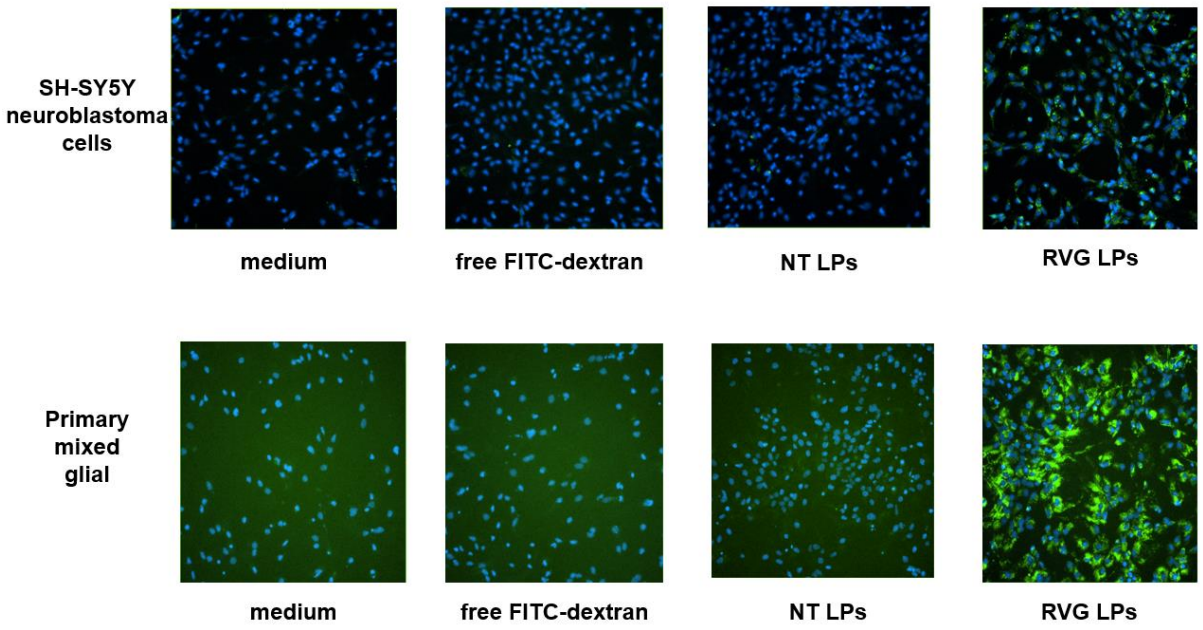


**Figure 5.** Free FITC-dextran, NT LPs and RVG LPs' cell uptake in SH-SY5Y neuroblastoma cells and mixed glial cells. The images show FITC-dextran (green) and nuclei staining with 40,6-diamidino-2-phenylindole (DAPI) (blue).

## Quantification of FITC-dextran

Typical calibration curves of FITC-dextran in DI water, plasma, and brain tissue homogenate are listed (Figure 6). As shown in the figure, the correlation coefficient (r) exceeded 0.99, showing good linearity over the concentration range. In DI water, FITC-dextran calibration curves were fitted over the concentration range of 0.005-5μM. The linear ranges of the calibration curves in plasma and brain homogenate were between 0.01-5μM and 0.03-0.5μM, respectively.

An efficient extraction procedure was developed which minimizes the interference of

the background's fluorescence intensity. The control group was prepared by spiking different concentrations of FITC-dextran to the supernatant collected from the blank plasma or brain homogenate after protein extraction. The efficiency of protein extraction was determined by comparing samples extracted from plasma or tissue homogenates with the control group.

The results showed that over 90% of FITC-dextran was extracted from plasma and the recoveries of FITC-dextran for the brain tissue homogenate were over 85%, which supports the method's validation.

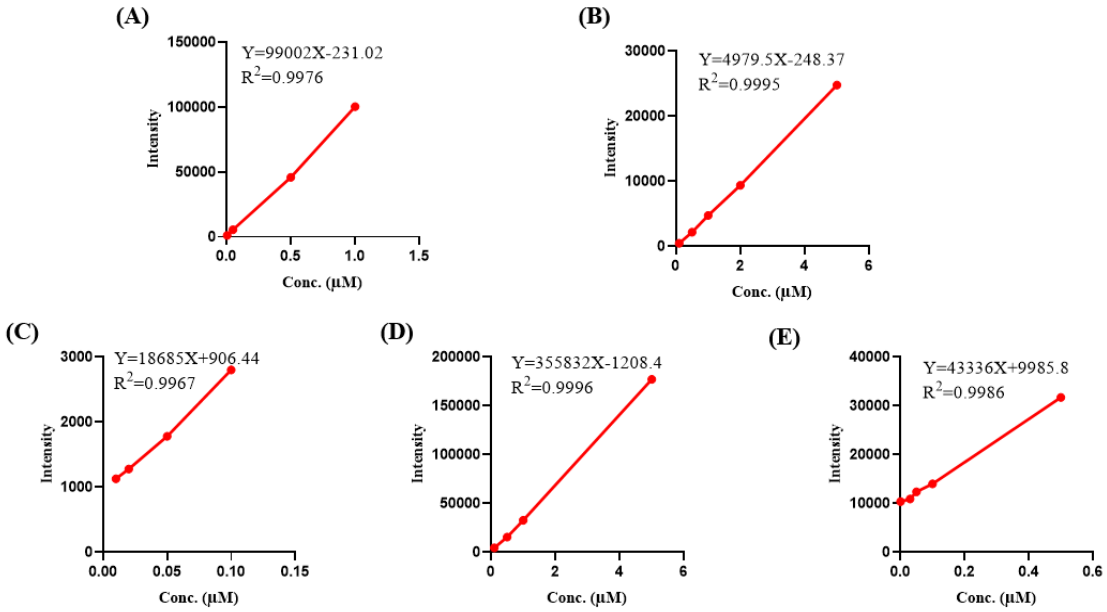


**Figure 6.** Calibration curves of FITC-dextran. (A) In DI water (0.005-1µM); (B) In DI water (1-5µM); (C) In plasma (0.01-0.1µM); (D) In plasma (0.1-5 µM); (E) In brain homogenate (0.03-0.5µM)

### *In vitro* release study

To serve as drug carriers and promote drug accumulation, it is crucial for liposomes to entrap the drug molecules for a prolonged period in circulation. Although the physiological environment in the human body is more complexed than *in vitro*, the evaluation of the drug

release profile is still an important aspect to predict the release kinetics *in vivo*. Here, the release kinetics of FITC-dextran from NT LPs was studied. The release of free FITC-dextran was examined as a control group to verify that the diffusion of drug molecules across the dialysis membrane was not a rate-limiting step during the release process. As illustrated in Table 2 and Figure 7, NT LPs had a significantly prolonged-release half-life ($t_{1/2}$, release, 41.7 hours), comparing to the free drug (3.72 hours).

Next, we carried out the release study in the presence of 90 % FBS to mimic the *in vivo* environment of drug circulation. As illustrated (Table 2, Figure 7), the release of FITC-dextran from NT LPs in 90% FBS was significantly slower ($t_{1/2}$, release, 27.65 h) than the free drug ($t_{1/2}$, release, 4.03 h). The presence of serum made the release of drug molecules from NT LPs faster overall, suggesting that serum proteins may influence NT LP's encapsulation ability.

**Table 2.** The release half-lives ($t_{1/2}$, release) of free FITC-dextran and NT LPs in PBS and 90% FBS

| Formulation | $t_{1/2}$, release (h) | The goodness of fit ($R^2$) |
|---|---|---|
| Free FITC-dextran in PBS | 3.72 | 0.9984 |
| Free FITC-dextran in 90% FBS | 4.03 | 0.9876 |
| NT LPs in PBS | 41.70 | 0.9254 |
| NT LPs in 90% FBS | 27.65 | 0.9011 |

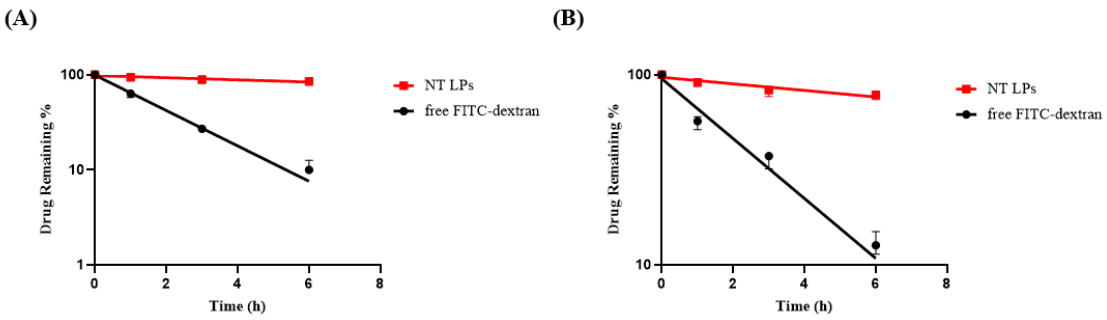


**Figure 7.** *In vitro* release profile of free FITC-dextran and NT LPs in PBS and 90% FBS. (A) Free FITC-dextran and NT LPs release study in PBS. (B) Free FITC-dextran and NT LPs release study in 90% FBS.

**Pharmacokinetics of free FITC-dextran and NT LPs**

The FITC-dextran concentration in plasma-time profiles of free FITC-dextran and NT LPs are illustrated in Figure 8. FITC-dextran concentration in plasma-time data with free FITC-dextran and NT LPs best fit a two-compartment model, characterized by an initial rapid phase of drug concentration decrease, and a slower terminal elimination phase. The pharmacokinetic parameters of free FITC-dextran and NT LPs are shown in Table 3. The AUC of free FITC-dextran was 16.55 μM*h, and the terminal half-life ($t_{1/2}$) was 0.71 hours. Additional pharmacokinetic parameters of NT LPs were an AUC of 22.50 μM*h and a terminal half-life ($t_{1/2}$) of 1.41 hours.

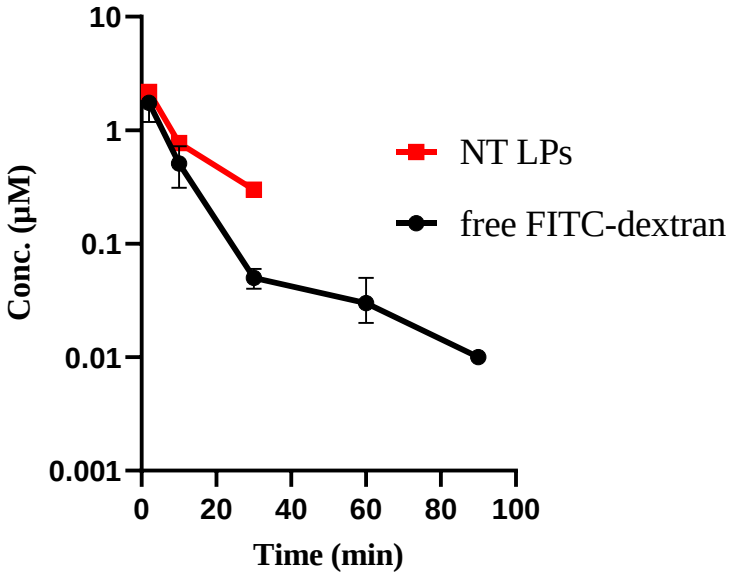


**Figure 8.** Pharmacokinetics of free FITC-dextran and NT LPs.

**Table 3.** The half-lives ($t_{1/2}$), the area under the curves (AUC) of free FITC-dextran and NT LPs for the intravenous injection

| | $t_{1/2}$(h) | AUC (μM*h) |
|---|---|---|
| free FITC-dextran | 0.71 | 16.55 |
| NT LPs | 1.41 | 22.50 |

**Brain distribution study**

The fluorescent signal in the brain homogenate of the mice that was intravenously injected with free FITC-dextran was 10361. It was almost equaled to the control group which was 10381. The result illustrated that there is almost no drug distributed in the brain. This was expected since free FITC-dextran is not able to pass through the BBB without the liposomal carriers.

## IV. DISCUSSION

The presence of the blood-brain barrier (BBB) is one of the major challenges of drug delivery to the brain. Liposome-based formulations have been investigated extensively as delivery systems to overcome the BBB. Utilization of the transporters expressed on the BBB has been an attractive strategy for the therapeutic delivery of drugs into the brain, and several carrier-mediated brains targeting drug delivery systems have been developed. Based on the fact that RVG can specifically interact with the nAchR which is widely expressed in the brain, we prepared an RVG-linked liposome. And a plain NT LPs without the target ligand was also prepared for comparison. The characteristics of the liposomal formulation were investigated.

Particle size and zeta potential are important factors that affect the liposome uptake by the brain capillary cells on the BBB, and the size distribution is generally limited within 200 nm in diameter for brain-targeted liposomes[31]. Liposomes being too small (size < 50 nm) may escape out of peripheral capillaries, while liposomes being too large (size > 200 nm) may not be able to pass cell membranes and may be removed faster by the reticuloendothelial system (RES). Particles below 200 nm avoid recognition by the RES and exhibit a prolonged half-life in the blood. In this study, NT LPs and RVG LPs were successfully prepared with particle sizes narrowly distributed around 100 nm in diameter. Zeta potential values were between -20 mV to -30 mV. *In vitro* uptake experiments in SH-SY5Y neuroblastoma cells as

well as primary brain mixed glial cells clearly showed the cell uptake of RVG LPs was much higher than NT LPs, indicating a clear targeting effect of RVG LPs. Evaluation of *in vitro* drug release profiles is an important aspect of the development of drug carriers. In this study, the release profiles of NT LPs and free FITC-dextran in both PBS and 90% FBS solutions were analyzed. The results demonstrate the sustained release of FITC-dextran from NT LPs. By compare to the release study in PBS, the presence of serum made the release of drug molecules from NT LPs faster overall, suggesting that serum proteins may influence NT LP's encapsulation ability. However the substance release of FITC dextran in both release study demonstrate that the liposome truly encapsulated FITC-dextran and can work as a drug carrier

The pharmacokinetics of free FITC-dextran and NT LPs, as well as the brain distribution study of free FITC-dextran, were investigated after intravenous injection. The results showed that although the plasma concentration maintained a detectable level until 1 hour after intravenous administration, there was almost no FITC-dextran distributed in the brain. This is expected since FITC-dextran is a large and hydrophilic molecule that is unable to pass through the BBB without carriers.

In summary, RVG LPs have demonstrated a strong targeting efficiency to the brain cells, it is reasonable to expect an enhanced brain distribution of payload by RVG LPs *in vivo*. Further evaluation of the pharmacokinetics and brain distribution study of NT LPs and RVG LPs are warranted.

# REFERENCES

1 Khan, A. R., Yang, X., Fu, M. & Zhai, G. Recent progress of drug nanoformulations targeting to brain. *J Control Release* **291**, 37-64, doi:10.1016/j.jconrel.2018.10.004 (2018).

2 Gustavsson, A. *et al.* Cost of disorders of the brain in Europe 2010. *Eur Neuropsychopharmacol* **21**, 718-779, doi:10.1016/j.euroneuro.2011.08.008 (2011).

3 Zhou, Y., Peng, Z., Seven, E. S. & Leblanc, R. M. Crossing the blood-brain barrier with nanoparticles. *J Control Release* **270**, 290-303, doi:10.1016/j.jconrel.2017.12.015 (2018).

4 Tang, W. *et al.* Emerging blood-brain-barrier-crossing nanotechnology for brain cancer theranostics. *Chem Soc Rev* **48**, 2967-3014, doi:10.1039/c8cs00805a (2019).

5 Dong, X. Current Strategies for Brain Drug Delivery. *Theranostics* **8**, 1481-1493, doi:10.7150/thno.21254 (2018).

6 Vieira, D. B. & Gamarra, L. F. Getting into the brain: liposome-based strategies for effective drug delivery across the blood-brain barrier. *Int J Nanomedicine* **11**, 5381-5414, doi:10.2147/IJN.S117210 (2016).

7 Bhaskar, S. *et al.* Multifunctional Nanocarriers for diagnostics, drug delivery and targeted treatment across blood-brain barrier: perspectives on tracking and neuroimaging. *Particle and Fibre Toxicology*, doi:org/10.1186/1743-8977-7-3 (2010).

8 Abbott, N. J., Patabendige, A. A., Dolman, D. E., Yusof, S. R. & Begley, D. J. Structure and function of the blood-brain barrier. *Neurobiol Dis* **37**, 13-25, doi:10.1016/j.nbd.2009.07.030 (2010).

9 Valentín Ceña , P. J. Nanoparticle crossing of blood–brain barrier: a road to new therapeutic approaches to central nervous system diseases. *Nanomedicine* (2018).

10 Rip, J., Schenk, G. J. & de Boer, A. G. Differential receptor-mediated drug targeting to the diseased brain. *Expert Opin Drug Deliv* **6**, 227-237, doi:10.1517/17425240902806383 (2009).

11 Chen, Y. & Liu, L. Modern methods for delivery of drugs across the blood-brain barrier. *Adv Drug Deliv Rev* **64**, 640-665, doi:10.1016/j.addr.2011.11.010 (2012).

12 Agrawal, M. *et al.* Recent advancements in liposomes targeting strategies to cross blood-brain barrier (BBB) for the treatment of Alzheimer's disease. *J Control Release* **260**, 61-77, doi:10.1016/j.jconrel.2017.05.019 (2017).

13 Ceña, V. & Játiva, P. Nanoparticle crossing of blood brain barrier a road to new therapeutic approaches to central nervous system diseases. *Nanomedicine*, doi:org/10.2217/nnm-2018-0139 (2018).

14 Bulbake, U., Doppalapudi, S., Kommineni, N. & Khan, W. Liposomal Formulations in Clinical Use: An Updated Review. *Pharmaceutics* **9**, doi:10.3390/pharmaceutics9020012 (2017).

15 Li, X., Ding, L., Xu, Y., Wang, Y. & Ping, Q. Targeted delivery of doxorubicin using stealth liposomes modified with transferrin. *Int J Pharm* **373**, 116-123, doi:10.1016/j.ijpharm.2009.01.023 (2009).

16 Ross, C., Taylor, M., Fullwood, N. & Allsop, D. Liposome delivery systems for the treatment of Alzheimer's disease. *Int J Nanomedicine* **13**, 8507-8522, doi:10.2147/IJN.S183117 (2018).

17 Tao, Y., Han, J. & Dou, H. Brain-targeting gene delivery using a rabies virus glycoprotein peptide

modulated hollow liposome: bio-behavioral study. *Journal of Materials Chemistry* **22**, doi:10.1039/c2jm31675g (2012).

18 Huey, R., Hawthorne, S. & McCarron, P. The potential use of rabies virus glycoprotein-derived peptides to facilitate drug delivery into the central nervous system: a mini review. *J Drug Target* **25**, 379-385, doi:10.1080/1061186X.2016.1223676 (2017).

19 Dos Santos Rodrigues, B., Arora, S., Kanekiyo, T. & Singh, J. Efficient neuronal targeting and transfection using RVG and transferrin-conjugated liposomes. *Brain Res* **1734**, 146738, doi:10.1016/j.brainres.2020.146738 (2020).

20 Kumar, P. *et al.* Transvascular delivery of small interfering RNA to the central nervous system. *Nature* **448**, 39-43, doi:10.1038/nature05901 (2007).

21 Chen, W. *et al.* Targeted brain delivery of itraconazole via RVG29 anchored nanoparticles. *J Drug Target* **19**, 228-234, doi:10.3109/1061186X.2010.492523 (2011).

22 Bommana, M. M., Kirthivasan, B. & Squillante, E. In vivo brain microdialysis to evaluate FITC-dextran encapsulated immunopegylated nanoparticles. *Drug Deliv* **19**, 298-306, doi:10.3109/10717544.2012.714812 (2012).

23 Hoffmann, A. *et al.* High and Low Molecular Weight Fluorescein Isothiocyanate (FITC)-Dextrans to Assess Blood-Brain Barrier Disruption: Technical Considerations. *Transl Stroke Res* **2**, 106-111, doi:10.1007/s12975-010-0049-x (2011).

24 Natarajan, R., Northrop, N. & Yamamoto, B. Fluorescein Isothiocyanate (FITC)-Dextran Extravasation as a Measure of Blood-Brain Barrier Permeability. *Curr Protoc Neurosci* **79**, 9 58 51-59 58 15, doi:10.1002/cpns.25 (2017).

25 Has, C. & Sunthar, P. A comprehensive review on recent preparation techniques of liposomes. *J Liposome Res*, 1-30, doi:10.1080/08982104.2019.1668010 (2019).

26 Wu, H. *et al.* Cholesterol-tuned liposomal membrane rigidity directs tumor penetration and anti-tumor effect. *Acta Pharm Sin B* **9**, 858-870, doi:10.1016/j.apsb.2019.02.010 (2019).

27 Tucci, S. T. *et al.* Tumor-specific delivery of gemcitabine with activatable liposomes. *J Control Release* **309**, 277-288, doi:10.1016/j.jconrel.2019.07.014 (2019).

28 Leibrand, C. R. *et al.* HIV-1 Tat and opioids act independently to limit antiretroviral brain concentrations and reduce blood-brain barrier integrity. *J Neurovirol* **25**, 560-577, doi:10.1007/s13365-019-00757-8 (2019).

29 Katragadda, U., Teng, Q., Rayaprolu, B. M., Chandran, T. & Tan, C. Multi-drug delivery to tumor cells via micellar nanocarriers. *Int J Pharm* **419**, 281-286, doi:10.1016/j.ijpharm.2011.07.033 (2011).

30 Kulkarni, S. A. & Feng, S. S. Effects of particle size and surface modification on cellular uptake and biodistribution of polymeric nanoparticles for drug delivery. *Pharm Res* **30**, 2512-2522, doi:10.1007/s11095-012-0958-3 (2013).

31 Kaur, I. P., Bhandari, R., Bhandari, S. & Kakkar, V. Potential of solid lipid nanoparticles in brain targeting. *J Control Release* **127**, 97-109, doi:10.1016/j.jconrel.2007.12.018 (2008).

# VITA

Ziru Zhang received her bachelor’s degree in pharmaceutics at Liaoning University of Traditional Chinese Medicine in 2017. With a huge interest in working on formulations and natural products, she applied for the master's program in the Department of Pharmaceutics and Drug Delivery at the University of Mississippi. She will graduate in May 2020 and would like to continue working on formulation study in her future career.